SCIENCE CHINA
Chemistry

• ARTICLES •
· SPECIAL TOPIC · Electrochromics

January 2017 Vol.60 No.1: 84–89
doi: 10.1007/s11426-016-0286-8

A newly-designed self-powered electrochromic window

Xingming Wu, Jianming Zheng & Chunye Xu*

Hefei National Laboratory for Physical Sciences at Microscale, CAS Key Laboratory of Soft Matter Chemistry, Department of Polymer Science and Engineering, University of Science and Technology of China, Hefei 230026, China

Received July 8, 2016; accepted September 4, 2016; published online December 5, 2016

By converting incident light into electric power, self-powered electrochromic window (SP-ECW) can achieve color change in electrochromic layer with no need for external voltage. In this work, a newly-designed SP-ECW is proposed for altering its color between deep blue and colorless state according to on/off state of incident light. The device consists of a working electrode with planar integration of photovoltaic (PV) and electrochromic (EC) elements on one electrode, a platinum counter electrode and a redox electrolyte comprising Br^-/Br_3^- couple. A high transmittance modulation of 41% at 582 nm is obtained. Electrical energy converted from light is not only sufficient to drive the device, but also can be outputted to the external circuit.

self-powered electrochromic window, redox electrolyte, poly(3,4-(2,2-dimethylpropylenedioxy)thiophene), transmittance modulation, light intensity

Citation: Wu X, Zheng J, Xu C. A newly-designed self-powered electrochromic window. *Sci China Chem*, 2017, 60: 84–89, doi: 10.1007/s11426-016-0286-8

1 Introduction

Electrochromism refers to the phenomenon that a material reversibly changes its color when subjected to an external voltage [1,2]. Over the past few decades, electrochromic windows (ECWs) based on electrochromic (EC) materials have attracted wide attention due to their potential applications in indoor energy saving by modulating solar radiation [3–5]. However, conventional ECWs are operated under an applied voltage, requiring additional circuit layout and power supply. To address this point, methods of integrating an internal potential have been implemented for achieving self-powering of an ECW.

It is widely accepted that solar energy is one of the most important renewable energy source available today. Photovoltaic components, which are typically based on amorphous silicon thin film solar cell and dye-sensitized solar cell (DSSC) techniques, have been introduced into ECWs [6–11]. By harvesting solar radiation and converting it into electric power, the so-called self-powered electrochromic window (SP-ECW) can change its optical property with no need for additional power supply.

The configuration of SP-ECW can be divided into two types. Some SP-ECW modules vertically incorporated the photovoltaic (PV) element in a single device [6,12–17] or as a tandem structure [18], while others arranged the PV element planarly beside the EC element [7–9,19].

In the former type, the attractive topic is the photoelectrochromic devices (PECDs) [6,20–22], which is a combination of DSSC and ECW techniques based on the compatible nature of the two. First PECD was reported by Bechinger *et al*. [6] in 1996. By substituting a WO_3 EC electrode for the Pt electrode in a typical DSSC, the electrons generated by excited dye molecules could transport to the WO_3 electrode through the external circuit, resulting in the electrochromic

*Corresponding author (email: chunye@ustc.edu.cn)

process of WO_3. This PECD only exhibited a transmittance modulation of 18%. Since then, efforts have been directed to improve the optical performance of PECD. Nevertheless, there exists the inherent drawback, as the intrinsic high visible absorption of PV element. Consequently, the devices could not be colorless in the bleached state and thereby the application in the building field is limited.

In the latter SP-ECW type, since the PV and EC elements are not arranged facing each other, the transmittance modulation can be enhanced. In 2012, Huang *et al.* [9] proposed a solution type amorphous silicon-based SP-ECW, exhibiting a transmittance modulation of 70% at 590 nm; however, the bleaching time was 160 min long. Later, they developed a printable SP-ECW with integration of polyelectrolyte based EC film and silicon thin film solar cell [19]. This device could switch its color between pale green and light blue with a transmittance modulation of 34% at 665 nm, and the bleaching time was 38.1 min. DSSC technique is also introduced into this SP-ECW type. Remarkable transmittance modulation, along with fast response times, was achieved [7,8,23]; still, the reported devices could not be colorless in the bleached state owing to the dark color of I^-/I_3^- electrolyte used.

Our group has been focusing on developing PECD performance. In 2012, we reported a PECD with a PProDOT-Me_2/Pt counter electrode [14]. The polymer EC material-based device achieved a transmittance modulation of 38% at 637 nm and the highest photovoltaic conversion efficiency of 1.12% in reported PECDs at the time. In 2016, by substituting Br^-/Br_3^- electrolyte for I^-/I_3^- electrolyte, we improved the transmittance modulation of PECD to 44.3%, which is the highest value in the reported polymer EC material-based PECDs [16]. Nevertheless, these PECDs are still colored in the bleached state. On this account, we herein propose a newly-designed SP-ECW based on a highly transparent electrolyte and a working electrode with planar integration of PV and EC elements. The device can reveal its color change between deep blue and colorless state with the states of incident light. We strongly believe that this kind of SP-ECW has a great application prospect in the industrial and architectural fields.

2 Experimental

2.1 Materials

Acetonitrile (99.8%), methanol (99.8%), propylene carbonate (PC, 99.7%), ferrocene (98%), lithium bromide (LiBr, 99%) and lithium perchlorate ($LiClO_4$, 99.99%) were obtained from Sigma-Aldrich (USA). Bromine (Br_2, 99.5%) was purchased from Sinopharm Chemical Reagent Co., Ltd (China). The monomer 3,4-(2,2-dimethylpropylenedioxy)thiophene (ProDOT-Me_2) was synthesized according to the reported literature [3]. Platisol T, Ti-Nanoxide HT and Ruthenium 535-4TBA were together obtained from Solaronix (Switzerland).

2.2 Preparation of working electrode

Fluorine-doped tin oxide (FTO) glasses were successively cleaned by de-ionized water and ethanol for 30 min under ultrasonic condition and then were dried at 110 °C. TiO_2 nanoparticle paste was coated onto FTO glass in strips using doctor-blade method. Three strips of Scotch tape were parallelly applied on the FTO glass substrate. Afterward, TiO_2 paste was spread onto the gap between the tape strips with a glass rod, and then the tapes were removed. After naturally air drying, the TiO_2 film was sintered at 500 °C for 45 min, presenting a thickness of 3 μm. The electrode was immersed into a 0.3 mM Ruthenium 535-4TBA methanol solution for 24 h in a glove box, and then it was gently rinsed with ethanol to remove unadsorbed dye molecules and was air dried. Afterward, the FTO glass coated with dye-sensitized TiO_2 nanoparticle film was immersed in the bath solution containing 0.01 M monomer and 0.1 M $LiClO_4$ in acetonitrile and was carried out electropolymerization of PProDOT-Me_2 film using a three-electrode system with a silver wire reference electrode in addition to a platinum sheet counter electrode. EC polymer was electropolymerized onto the blank area of FTO glass at a constant potential of 1.7 V for 4 s. Electropolymerization of EC monomer did not occur on the dye/TiO_2 area. Finally the film was rinsed with ethanol gently and dried in atmosphere. The EC film presented a thickness of 180 nm. The preparation procedure is schematically shown in Figure 1.

2.3 Preparation of counter electrode

Liquid platinum precursor (Platisol T) was spread onto a clean FTO glass with spin coating method and then it was gradually heated at 110 °C for 30 min and at 450 °C for 30 min in a muffle furnace.

2.4 Assembly of the SP-ECW

The Br^-/Br_3^- redox electrolyte was prepared by mixing 0.3 M

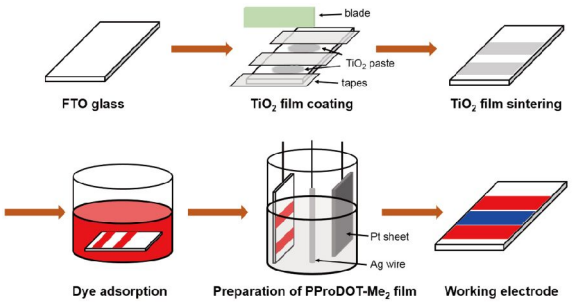

Figure 1 Schematic of preparation procedure of working electrode (color online).

LiBr and 2 mM Br_2 in propylene carbonate (PC) under nitrogen atmosphere in a glove box. The SP-ECW was assembled by sandwiching the working electrode and the counter electrode with the redox electrolyte. A schematic figure of the SP-ECW is shown in Figure 2.

2.5 Characterization

The surface morphology of PProDOT-Me_2 film was measured by scanning electron microscopy (SEM; Sirion 200, FEI, USA). Electropolymerization and cyclic voltammograms were performed on an electrochemical workstation (CHI 660D, CH Instruments, China) at room temperature. The $E^{0'}$ ($E^{0'}=(E_{ox}+E_{red})/2$) of the ferrocene-ferrocenium (F_c/F_c^+) couple was measured to be 0.33 V versus the silver wire in acetonitrile. Thicknesses of TiO_2 and EC films were determined using a surface profiler (Dektak, Veeco, USA). The transmittance spectra were recorded with a UV-Vis-NIR spectrophotometer (V-670, Jasco, Japan). The optical performances of SP-ECW were measured using a spectrometer (USB 2000+, Ocean Optics, USA). All the optical measurements are measured taking air as the reference spectrum. A 150 W halogen lamp was served as a light source for powering SP-ECW. The light intensity was calibrated using a radiometer (FZ-A, Photoelectric Instrument Factory of Beijing Normal University, China). The photovoltaic performance of SP-ECW was measured by a solar simulator (OTENTO-SUN II, Bunkoukeik Co., Ltd., Japan).

3 Results and discussion

3.1 Characterization of PProDOT-Me_2 film and Br^-/Br_3^- electrolyte

The PProDOT-Me_2 film deposited on FTO glass substrate exhibited a highly porous microstructure composed of 3D interconnected nanofibers (Figure 3(a)). The diameters of polymer fibers are approximately 40–60 nm. The porous structure allows PProDOT-Me_2 film to fully contact with the redox electrolyte and thereby the intercalation/extraction process of ions would be facilitated. Cyclic voltammogram (CV) of PProDOT-Me_2 film was measured in the PC solution containing 0.1 M $LiClO_4$ at a scan rate of 50 mV s^{-1} (Figure 3(b)). The oxidation and reduction peaks are at 0.08 and –0.23 V, respectively. During the cycling, the electrochromic phenomenon of PProDOT-Me_2 film could be observed. The film was transparent in the oxidized state and switched to the deep-blue state when it got reduced. The coloration efficiency (CE) is also an important parameter of EC material, which is defined as:

$$CE = \Delta OD / Q = \log(T_b / T_c) / Q \quad (1)$$

wherein Q represents the intercalated charge per unit area, T_b and T_c are the transmittances in the bleached and colored states, respectively. The coloration efficiency curve of PProDOT-Me_2 film at 582 nm under –1.2 V bias is shown in Figure 3(c) and the CE value is calculated to be 197.4 cm^2 C^{-1}. Our previous study shows that Br^-/Br_3^- electrolyte has little light absorption in the visible region [16]. Thus, the color of SP-ECW in the bleaching state will not be influenced by Br^-/Br_3^- electrolyte.

The CV curve of Br^-/Br_3^- electrolyte at a scan rate of 50

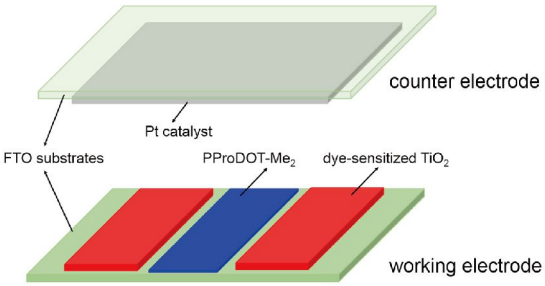

Figure 2 Schematic diagram of newly-designed SP-ECW. Inside working electrode is of planar integration of PV and EC elements (color online).

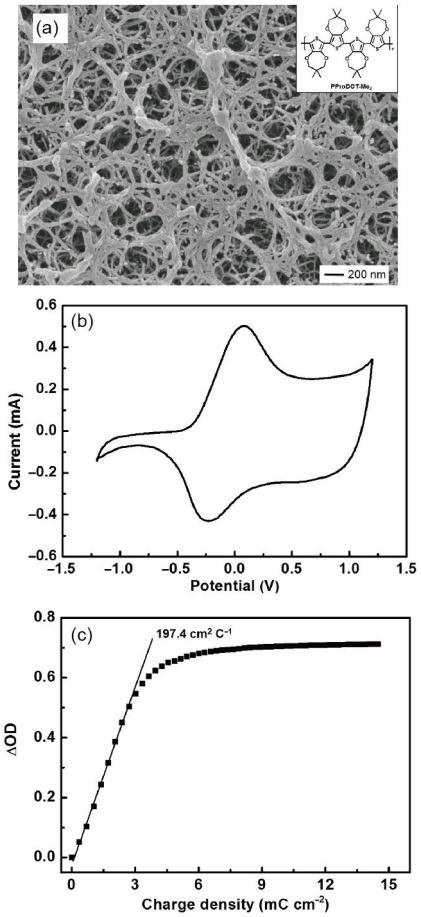

Figure 3 (a) SEM image of PProDOT-Me_2 film on FTO glass substrate (inset is the chemical structure of PProDOT-Me_2); (b) cyclic voltammetry curve of PProDOT-Me_2 film; (c) coloration efficiency of PProDOT-Me_2 film at 582 nm under –1.2 V bias.

mV s^{-1} is shown in Figure 4(a). Two pairs of redox peaks can be attributed to the redox reactions:

$$3Br^- \quad Br_3^- + 2e^- \tag{2}$$

$$2Br_2 + 2e^- \quad 2Br_3^- \tag{3}$$

Potentials of two oxidation peaks are at 1.03 and 1.33 V, respectively. And potentials of two reduction peaks are at 0.25 and 1.10 V, respectively.

CV results indicate that PProDOT-Me_2 film can be oxidized by Br^-/Br_3^- electrolyte. To visually investigate the oxidizing ability of Br^-/Br_3^- electrolyte to PProDOT-Me_2 film, we immersed colored PProDOT-Me_2 film (in reduced state) in Br^-/Br_3^- electrolyte (Figure 4(b)). Since PProDOT-Me_2 is an electrochromic material, the color change of the polymer is relevant to its redox state. In our experiment, once the PProDOT-Me_2 film was brought in contact with Br^-/Br_3^- electrolyte, the film was bleached immediately, indicating an oxidization process. The result demonstrates that Br^-/Br_3^- electrolyte possesses a strong oxidizing ability to PProDOT-Me_2 film.

3.2 Optical performance of SP-ECW

When the device is illuminated, electrons produced by dye molecules transfer to the conduction band of TiO_2, and gather on FTO glass surface, then diffuse into EC film. Correspondingly, EC film is reduced and changed into blue color (Figure 5(a)). When the device is under dark condition, no more electrons are produced again, while Br_3^- ions existing in the electrolyte can capture electrons in EC film because

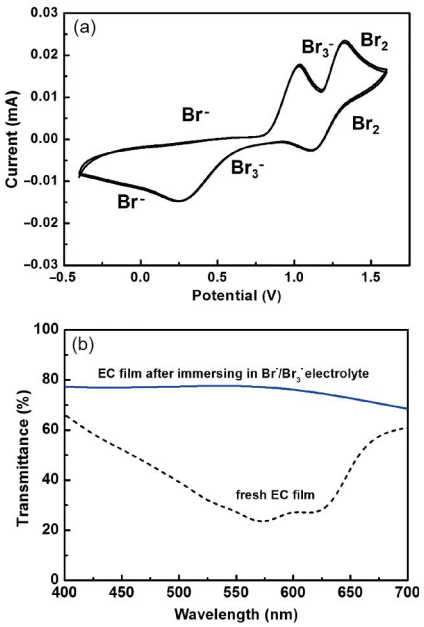

Figure 4 (a) Cyclic voltammetry curve of Br^-/Br_3^- electrolyte; (b) transmittances of PProDOT-Me_2 film in the colored state and after immersing in Br^-/Br_3^- electrolyte.

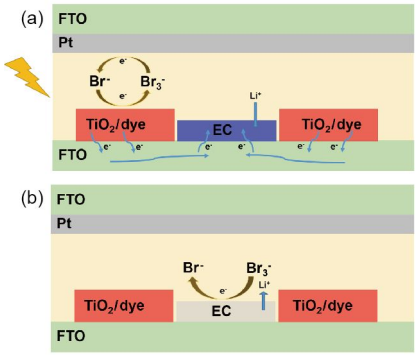

Figure 5 Schematic representation of the device operation process (a) under illumination and (b) in dark condition (color online).

of its oxidizing ability to EC film, leading to the bleaching process of EC film (Figure 5(b)).

Since the EC part only faces the highly transparent components such as FTO glass, redox electrolyte and Pt counter electrode (Figure 6) through the device thickness direction, the color change of device is mainly determined by the electrochromic property of EC material. Figure 7 shows the transmittance modulation of SP-ECW. For the new one, transmittance of the device in the bleached state was between 56% and 64% in the visible region, and transmittance in the colored state showed a minimum value of 22.4% at 582 nm. The maximum transmittance modulation was 41% at 582 nm. To investigate the cycling stability of the SP-ECW, we repeatedly cycled the device through switching on and off states of incident light. It can be seen that after 100 cycles, transmittance of device in the bleached state showed little change, while transmittance in the colored state showed a minimum value of 23.6% at 582 nm. The device exhibited a maximum transmittance modulation of 40% at 582 nm. Figure 7 also shows the photographs of a device with total dye area of 5.6 cm^2 and EC area of 3.6 cm^2 in the bleached and colored states. Since the dye part is not arranged facing the EC part, additionally, the Br^-/Br_3^- electrolyte used has little absorption in visible region, the SP-ECW could be colorless in the bleached state, which would be a great advantage over other reported SP-ECW modules in building applications.

Figure 8 shows the *in-situ* transmittance change of the device. The time altering its 95% transmittance modulation between the bleached and colored states is defined as the response time here. With light on, the transmittance of device decreased with a response time of 26 s from a fully bleached state. With light off, the EC film was bleached under the oxidizing effect of redox electrolyte. The transmittance increased with a response time of 7 s. After 100 cycles, the response times for both coloring and bleaching processes showed little change, demonstrating a good stability.

Figure 9 shows the CIE 1931 color space colorimetry of SP-ECW. The chromaticity coordinates (x, y, Y_L%) of device

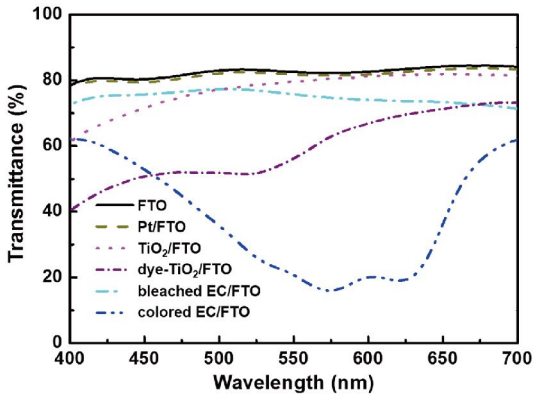

Figure 6 Transmittances of all components in SP-ECW (color online).

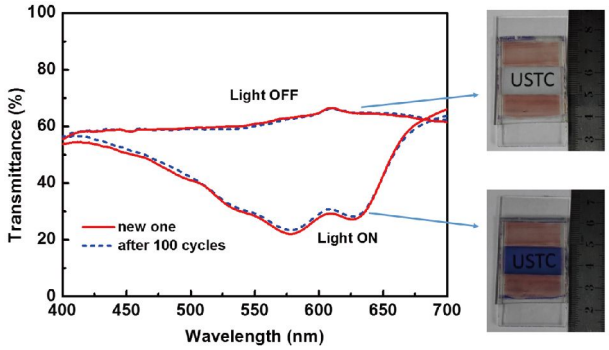

Figure 7 Transmittance modulation of SP-ECW. Insets are photos of a device in the bleached and colored states (color online).

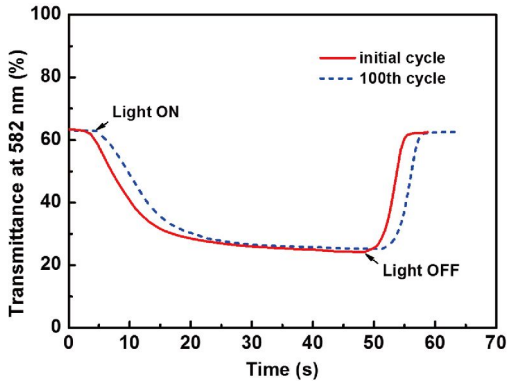

Figure 8 *In-situ* transmittance change of SP-ECW. The solid line represents the initial cycle and the short-dashed line represents the 100th cycle.

changes from (x=0.3196, y=0.3375, Y_L%=73.36%) at bleached state to (x=0.2569, y=0.2595, Y_L%=32.57%) at colored state. This further proves that the SP-ECW alters its color between deep blue and colorless state.

In practical application, solar radiation reaching a building is influenced by climatic conditions and seasons. If the building is in winter or in high-latitude region, it is difficult for a building to be exposed to 1 sun power density. In view of this situation, we measured the *in-situ* transmittance change of the device at 582 nm under different illuminations of 30, 50, 70 and 100 mW cm^{-2}. As shown in Figure 10, with decreased light intensity, the response time for coloring process increased. Under illumination of 100 mW cm^{-2}, the device showed a response time for coloring process of 26 s. Under illumination of 70 mW cm^{-2}, the coloring time increased to 68 s. Under illuminations of 50 and 30 mW cm^{-2}, the coloring time increased to 85 and 95 s, respectively. Furthermore, the device could finally achieve the same coloring depth of 24% at 582 nm under illuminations of 50, 70 and 100 mW cm^{-2}, whereas the device reached a lighter coloring depth of 32% at 582 nm under illumination of 30 mW cm^{-2}. Under illumination less than 30 mW cm^{-2}, we found that the device could not be colored, since there were insufficient photogenerated electrons for driving the coloring process.

3.3 Photovoltaic performance of SP-ECW

After the EC film was colored, the SP-ECW could further output the net electrical power in addition to operating the electrochromic process. The measured current-voltage (I-V) characteristic of the device at AM 1.5 (100 mW cm^{-2}) is shown in Figure 11. The short-circuit density (J_{sc}) value was

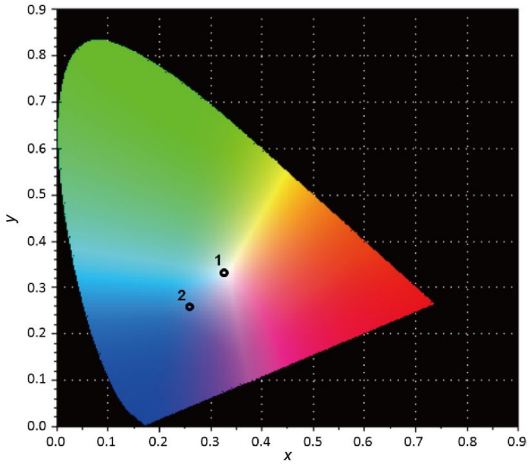

Figure 9 CIE 1931 color space colorimetry of device (1) in bleached state and (2) in colored state (color online).

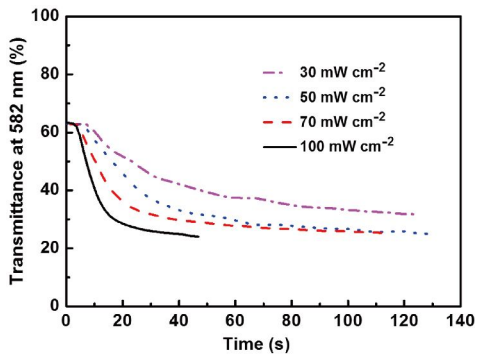

Figure 10 *In-situ* transmittance change of SP-ECW under different light intensity (color online).

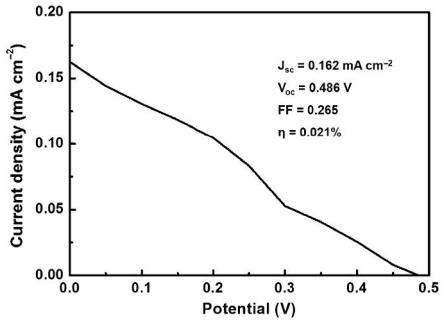

Figure 11 Photovoltaic performance of SP-ECW under AM 1.5 (100 mW cm^{-2}).

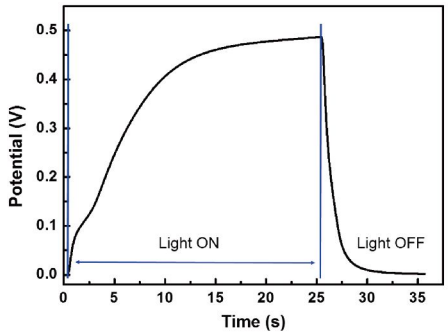

Figure 12 Evolution of the potential of SP-ECW in an open-circuit condition (color online).

0.162 mA cm^{-2}, the open-circuit voltage (V_{oc}) value was 0.486 V, the fill factor (FF) was 0.265, and the overall photovoltaic conversion efficiency (η) was 0.021%. The low FF may be ascribed to the charge recombination at the photoanode/electrolyte interface since the dye/TiO_2 did not cover the photoanode completely. Under illumination less than 100 mW cm^{-2}, the η value was even lower. The device photovoltage value generated in an open-circuit condition is also measured (Figure 12). When the SP-ECW is illuminated, the potential increased and approached the V_{oc} of device within 25 s. When the device is in dark condition, the potential decreased to 0 V within about 7 s, which is quite consistent with the bleaching time of device. The photovoltaic performance of the SP-ECW in this work is still unsatisfactory, investigating other dyes and redox couples for improving the photovoltaic performance of the device will be conducted in our next work.

4 Conclusions

In this paper, we presented a newly-designed self-powered electrochromic window based on a highly transparent electrolyte and a planarly integrated working electrode. Under illumination, the device can convert incident light into electric power for driving the electrochromism of EC film, turning into deep-blue color. Under dark condition, the device turns to colorless state owing to the strong oxidizing ability of Br^-/Br_3^- electrolyte to EC film. The device achieves a transmittance modulation of 41% at 582 nm under 100 mW cm^{-2}, with a coloring time of 26 s and a bleaching time of 7 s. A good cycling stability over 100 cycles is also obtained. Light intensity also shows impact on the coloring process of device, with increased light intensity, the coloring speed increases. Furthermore, the SP-ECW can output the net electrical power in addition to operating the EC process. We believe that the SP-ECW proposed here has a promising potential in building application.

Acknowledgments This work was supported by the National Natural Science Foundation of China (21274138, 21273207, 21474096) and the Chinese Academy of Sciences (Integrated system of high efficiency building energy saving and its application, KFZD-SW-403).

Conflict of interest The authors declare that they have no conflict of interest.

1 Lampert CM. *Solar Energy Mater*, 1984, 11: 1–27
2 Rosseinsky DR, Mortimer RJ. *Adv Mater*, 2001, 13: 783–793
3 Xu C, Liu L, Legenski SE, Ning D, Taya M. *J Mater Res*, 2004, 19: 2072–2080
4 Argun AA, Aubert PH, Thompson BC, Schwendeman I, Gaupp CL, Hwang J, Pinto NJ, Tanner DB, MacDiarmid AG, Reynolds JR. *Chem Mater*, 2004, 16: 4401–4412
5 Yang S, Zheng J, Wu X, Xu C. *Acta Chim Sin*, 2013, 71: 1041–1046
6 Bechinger C, Ferrere S, Zaban A, Sprague J, Gregg BA. *Nature*, 1996, 383: 608–610
7 Wu JJ, Hsieh MD, Liao WP, Wu WT, Chen JS. *ACS Nano*, 2009, 3: 2297–2303
8 Cannavale A, Manca M, Malara F, De Marco L, Cingolani R, Gigli G. *Energy Environ Sci*, 2011, 4: 2567–2574
9 Huang LM, Hu CW, Liu HC, Hsu CY, Chen CH, Ho KC. *Sol Energ Mat Sol C*, 2012, 99: 154–159
10 Deb SK, Lee SH, Edwin Tracy C, Roland Pitts J, Gregg BA, Branz HM. *Electrochim Acta*, 2001, 46: 2125–2130
11 Gao W, Liu P, Crandall RS, Lee SH, Benson DK, Branz HM. *J Non-Cryst Solids*, 2000, 266: 1140−1144
12 De Filpo G, Mormile S, Nicoletta FP, Chidichimo G. *J Power Sources*, 2010, 195: 4365–4369
13 Leftheriotis G, Syrrokostas G, Yianoulis P. *Sol Energ Mat Sol C*, 2010, 94: 2304–2313
14 Yang S, Zheng J, Li M, Xu C. *Sol Energ Mat Sol C*, 2012, 97: 186–190
15 Cannavale A, Manca M, De Marco L, Grisorio R, Carallo S, Suranna GP, Gigli G. *ACS Appl Mater Interfaces*, 2014, 6: 2415–2422
16 Wu X, Zheng J, Xu C. *Electrochim Acta*, 2016, 191: 902–907
17 Chen M, Yang S, Zheng J, Xu C. *Acta Chim Sin*, 2013, 71: 713–716
18 Dyer AL, Bulloch RH, Zhou Y, Kippelen B, Reynolds JR, Zhang F. *Adv Mater*, 2014, 26: 4895–4900
19 Huang LM, Hu CW, Peng CY, Su CH, Ho KC. *Sol Energ Mat Sol C*, 2016, 145: 69–75
20 Hauch A, Georg A, Baumgärtner S, Opara Krašovec U, Orel B. *Electrochim Acta*, 2001, 46: 2131–2136
21 Hsu CY, Lee KM, Huang JH, Justin Thomas KR, Lin JT, Ho KC. *J Power Sources*, 2008, 185: 1505–1508
22 Jiao Z, Song JL, Sun XW, Liu XW, Wang JM, Ke L, Demir HV. *Sol Energ Mat Sol C*, 2012, 98: 154–160
23 Bella F, Leftheriotis G, Griffini G, Syrrokostas G, Turri S, Grätzel M, Gerbaldi C. *Adv Funct Mater*, 2016, 26: 1127–1137